Received: 13 January 2022 | Revised: 11 March 2022 | Accepted: 23 March 2022

DOI: 10.1002/bdr2.2009

Birth Defects Research | Society for Birth Defects Research & Prevention | WILEY

RESEARCH ARTICLE

The pro-apoptotic *Bax* gene modifies susceptibility to craniofacial dysmorphology following gastrulation-stage alcohol exposure

Eric W. Fish[1] | **Haley N. Mendoza-Romero**[1] | **Charlotte A. Love**[1] | **Constance J. Dragicevich**[1] | **Michael D. Cannizzo**[1] | **Karen E. Boschen**[1] | **Austin Hepperla**[2,3] | **Jeremy M. Simon**[2,3,4] | **Scott E. Parnell**[1,2,5]

[1]Bowles Center for Alcohol Studies, University of North Carolina, Chapel Hill, North Carolina, USA

[2]Carolina Institute for Developmental Disabilities, University of North Carolina, Chapel Hill, North Carolina, USA

[3]Neuroscience Center, University of North Carolina, Chapel Hill, North Carolina, USA

[4]Department of Genetics, University of North Carolina, Chapel Hill, North Carolina, USA

[5]Department of Cell Biology and Physiology, University of North Carolina, Chapel Hill, North Carolina, USA

Correspondence
Scott E. Parnell, Bowles Center for Alcohol Studies, University of North Carolina; Carolina Institute for Developmental Disabilities, University of North Carolina; Department of Cell Biology and Physiology, University of North Carolina. Thurston-Bowles, 104 Manning Dr. CB# 7178, UNC-Chapel Hill, Chapel Hill, NC 27599, USA.
Email: sparnell@med.unc.edu

Funding information
Eunice Kennedy Shriver National Institute of Child Health and Human Development, Grant/Award Number: U54-HD079124; National Institute of Neurological Disorders and Stroke, Grant/Award Number: P30NS045892; National Institute on Alcohol Abuse and Alcoholism, Grant/Award Number: U01-AA021651

Abstract

Background: During early development, alcohol exposure causes apoptotic cell death in discrete regions of the embryo which are associated with distinctive patterns of later-life abnormalities. In gastrulation, which occurs during the third week of human pregnancy, alcohol targets the ectoderm, the precursor of the eyes, face, and brain. This midline tissue loss leads to the craniofacial dysmorphologies, such as microphthalmia and a smooth philtrum, which define fetal alcohol syndrome (FAS). An important regulator of alcohol-induced cell death is the pro-apoptotic protein Bax. The current study determines if mice lacking the *Bax* gene are less susceptible to the pathogenic effects of gastrulation-stage alcohol exposure.

Methods: Male and female $Bax^{+/-}$ mice mated to produce embryos with full ($^{-/-}$) or partial ($^{+/-}$) *Bax* deletions, or $Bax^{+/+}$ wild-type controls. On Gestational Day 7 (GD 7), embryos received two alcohol (2.9 g/kg, 4 hr apart), or control exposures. A subset of embryos was collected 12 hr later and examined for the presence of apoptotic cell death, while others were examined on GD 17 for the presence of FAS-like facial features.

Results: Full *Bax* deletion reduced embryonic apoptotic cell death and the incidence of fetal eye and face malformations, indicating that Bax normally facilitates the development of alcohol-induced defects. An RNA-seq analysis of GD 7 $Bax^{+/+}$ and $Bax^{-/-}$ embryos revealed 63 differentially expressed genes, some of which may interact with the *Bax* deletion to further protect against apoptosis.

Conclusions: Overall, these experiments identify that Bax is a primary teratogenic mechanism of gastrulation-stage alcohol exposure.

KEYWORDS

apoptosis, ethanol, eye defects, fetal alcohol syndrome, knockout mouse, RNA-sequencing

1 | INTRODUCTION

Prenatal alcohol exposure (PAE) is one of the most preventable causes of birth defects. However, fetal alcohol spectrum disorders (FASD) are common; conservative estimates among first graders in the United States ranged between 1 and 5%, and less conservative estimates found as many as 9% of children had FASD (May et al., 2018). The most severe FASD is fetal alcohol syndrome (FAS) which is characterized by distinctive craniofacial appearances that fall within the holoprosencephaly spectrum, including a small or undefined philtrum, a thin upper lip, narrowly spaced eyes, epicanthal folds, short palpebral fissures, microphthalmia, and to a lesser extent, small lower jaws and overall flat midface (Del Campo & Jones, 2017). PAE also alters several brain structures and central nervous system functions that cause people with FAS to have cognitive and socio-emotional difficulties (Kelly, Day, & Streissguth, 2000; Mattson, Crocker, & Nguyen, 2011; Streissguth et al., 1991). These craniofacial and brain malformations are due to alcohol exposures during the gastrulation stage of development, which takes place during the third week of pregnancy, a time when many pregnancies are still unrecognized.

One of the challenges to understanding the etiology of FASD is that PAE affects people differently and not all exposures result in recognizable FASD. In fact, only an estimated 4.3% of children will develop FAS following heavy alcohol exposure (Abel, 1995). Like other teratogenic exposures, the amount, duration, and timing of PAE are factors that are often difficult to discern in clinical studies, but that will nonetheless influence developmental outcomes (Petrelli, Weinberg, & Hicks, 2018). Moreover, genetic factors are very important in FASD, as highlighted by a study in alcohol-exposed twins that found that 60% of dizygotic twins had identical diagnoses of FAS and similar IQ scores, while monozygotic twins were 100% concordant for these traits (Streissguth & Dehaene, 1993). These findings of broad genetic influences on PAE outcomes are supported by animal studies demonstrating species and strain differences in response to PAE, as well as those that reveal the role of specific single genes (see, Eberhart & Parnell, 2016; Karacay & Bonthius, 2015). These single gene manipulation studies are also able to uncover the precise mechanisms by which PAE can perturb development and delineate those genes that are protective, and those which confer vulnerability to PAE.

Excessive embryonic cell death is a major pathogenic mechanism for defects caused by PAE. During the gastrulation stage (Gestational Day 17–20 in human pregnancy), PAE targets the ectodermal tissue that is destined to become the face and the brain, causing apoptosis (Dunty Jr., Chen, Zucker, Dehart, & Sulik, 2001) and disrupting vital cell signaling pathways, including Sonic hedgehog (Shh; Ahlgren, Thakur, & Bronner-Fraser, 2002; Boschen, Fish, & Parnell, 2021; Hong & Krauss, 2012; Zhang, Ojiaku, & Cole, 2013). Embryonic apoptosis is caused largely by caspase activation following permeabilization of the mitochondrial outer membrane (MOM), as opposed to activation of death receptors through the extrinsic pathway (Voss & Strasser, 2020). Bax (Bcl-2-like protein 4) is a pro-apoptotic effector protein that, like its partner Bak (Bcl-2-antagonist/killer 1), mediates the MOM potential. Bax is a normally inactive monomer prevented from accumulating in the mitochondria by the anti-apoptotic protein Bcl-2. Cytotoxic stimuli activate pro-apoptotic triggers, such as Bad, Puma, and Noxa, which alleviate the repression of Bax by inhibiting Bcl-2, and by directly activating Bax itself. Bax activation involves several conformational changes that allow it to join the mitochondrial membrane and oligomerize to form pores that disrupt the MOM (Pena-Blanco & Garcia-Saez, 2018).

The objective of the current study was to determine if mice lacking the *Bax* gene are protected from the effects of gastrulation-stage alcohol exposure. Full loss of the *Bax* gene is not lethal and the mice develop without any major developmental abnormalities, although $Bax^{-/-}$ male mice are infertile (Knudson, Tung, Tourtellotte, Brown, & Korsmeyer, 1995). More subtle effects of *Bax* deletion have been observed, particularly in the brain and eye, including increased neuronal number (Deckwerth et al., 1996; White, Keller-Peck, Knudson, Korsmeyer, & Snider, 1998), absence of size differences in two sexually dimorphic nuclei (Forger & Peskin, 2005), cerebellar migration defects (Jung et al., 2008), increased retinal cell numbers, glial cell density, and altered microglial shape (Kawai et al., 2009; Mac Nair, Schlamp, Montgomery, Shestopalov, & Nickells, 2016; Mosinger Ogilvie, Deckwerth, Knudson, & Korsmeyer, 1998). Importantly, *Bax* deficiency reduces neuronal and retinal cell death resulting from various injuries (Deckwerth et al., 1996; Robinson, Conley, & Kern, 2003; Semaan, Li, & Nickells, 2010; W. Sun & Oppenheim, 2003), including alcohol exposure. The role of Bax in FASD has been explored in third trimester-equivalent models of cerebellar and neocortical cell death (Britton & Miller, 2018; Heaton, Paiva, Madorsky, Siler-Marsiglio, & Shaw, 2006; Young et al., 2003); in each of these models, *Bax* deletion protects against neuronal loss. However, it is unclear whether Bax plays a role in alcohol-induced cell death occurring during gastrulation, before the onset of neurogenesis. We hypothesized *Bax* deletion would protect mice from developing gastrulation alcohol-induced craniofacial and brain dysmorphologies.

2 | METHODS

2.1 | Animals

Female and male mice on a C57BL/6 background, heterozygous for a *Bax* gene deletion were bred in the laboratory from founders generously donated by Mohanish Deshmukh (UNC Chapel Hill, originally obtained from Dr Stanley Korsmeyer (Knudson et al., 1995)). Timed pregnancies were established by housing one or two nulliparous female $Bax^{+/-}$ mice with one $Bax^{+/-}$ male for 1–2 hr. Gestational day (GD) 0 was defined as the beginning of the breeding period in which a copulation plug was detected. All mice lived in ventilated, polycarbonate cages containing a polycarbonate hut, nesting material, and cob bedding. Food (Purina Isopro RMH 3000, Purina, St. Louis, MO) and water were freely available through a wire food hopper and a drinking spout. The vivarium was 21 ± 1 °C and 30–40% humidity and had a 12:12 light: dark cycle (lights on at 7:00 a.m.). All experiments followed the NIH guidelines using methods approved by the IACUC of University of North Carolina at Chapel Hill.

2.2 | Genotyping protocol

Genotyping for *Bax* DNA was performed on tail or embryonic tissue using the primers: mutant forward CCG CTT CCA TTG CTC AGC GG; wild-type forward GAG CTG ATC AGA ACC ATC ATG; common GTT GAC CAG AGT GGC GTA GG.

2.3 | Prenatal alcohol exposure

Pregnant dams were housed in groups no larger than five. At GD 7, they received two intra-peritoneal (i.p.) injections of 25% ethanol (v/v in lactated Ringer's solution, LRS; $n = 33$ dams) at a 2.9 g/kg dose, given 4 hr apart. This dosing caused peak blood alcohol levels of ∼445 ± 29 (*SEM*) mg/dl, taken 30 min after the second injection from ∼30 μl of tail blood analyzed using the Analox AM1 (Analox Instruments, Toronto, ON). Control dams ($n = 28$) were injected similarly with the vehicle alone (1.5 ml/100 g body weight).

2.4 | Nile blue experiments

On GD 7.5 (12 hr after alcohol), control and PAE embryos were collected following euthanasia of the dam. Embryos were dissected from extra-embryonic membranes in 37°C LRS and the numbers of live, dead, or resorbed embryos in each uterus were recorded. Nile Blue working solution [1:10,000] was warmed to 37°C in flat-bottom tubes prior to embryo immersion. Embryos were incubated for 30 min in the 37°C oven then rinsed briefly in LRS. Finally, specimens were photographed in LRS and genotyped.

2.5 | Morphology experiments

On GD 17, fetuses were collected after CO_2 asphyxiation and physical euthanasia of the dam. Fetuses were examined for facial and ocular malformations and tail samples were obtained for genotyping. Based on externally visible malformations, subsets of fetuses were drop-fixed in either 10% buffered formalin or first photographed by a MicroPublisher 5.0 digital camera (QImaging, British Columbia, Canada) on a Nikon SMZ–U Stereoscopic Zoom dissecting microscope (Nikon Corporation, Melville, NY) using QCapture Suite software, and then drop-fixed in Bouin's fixative. Ocular malformations were evaluated, either at the time of dissection or later in formalin-fixed specimens, by two independent evaluators who were blinded to treatment and genotype, using a 7-point dysmorphology scale modified from Parnell et al. (2006); Parnell, Sulik, Dehart, and Chen (2010) and Gilbert et al. (2016). A score for each eye was assigned based on the following criteria: (a) normal globe size, normally shaped pupil; (b) mildly microphthalmic or abnormally shaped (but noncolobomatous) pupil; (c) mildly microphthalmic with small, abnormally shaped (but noncolobomatous) pupil; (d) moderately microphthalmic with iridio-retinal coloboma; (e) severely microphthalmic with iridio-retinal coloboma; (f) severely microphthalmic, absent pupil; (g) apparently anophthalmic. For each fetus, the score that reflected the more dysmorphic eye was used for analyses. Image J software (https://imagej.nih.gov/ij/) was used to measure the size of the lens and globe from a subset of photographed fetuses. Heads of Bouin's fixed specimens were cleared with 70% ethanol, then processed using a Leica brand tissue processor and embedded in paraffin. Serial 10-μm coronal sections were cut using a rotary microtome, mounted onto glass slides, and stained with hematoxylin and eosin (H&E). Stained sections were examined using an Olympus BX60 light microscope.

2.6 | Statistical analysis

Data on litter size and number of resorptions were analyzed with *t* tests, while Chi-square tests compared the proportion of fetuses with eye defects. Eye and globe sizes

were compared with one-way analysis of variance (ANOVA). Fetal dysmorphology data were considered significant at the $p < .05$ level. RNA-seq comparisons were considered significant with an adjusted $p < .05$.

2.7 | RNA isolation

On GD 7, untreated $Bax^{+/-}$ dams were euthanized as above. Under RNAse-free conditions, the embryos were dissected from the placentas and staged for developmental age (see, Boschen, Ptacek, Berginski, Simon, & Parnell, 2021). GD 7-aged embryos were freed from their extra-embryonic tissue and placed in RLT Plus Lysis Buffer (Qiagen, Germantown, MD) plus β-mercaptoethanol and stored at −80°C. Extra-embryonic tissue was placed into 14 ul of DNA lysis buffer (Allele-In-One Mouse Tail Direct Lysis Buffer, Allele Biotechnology, San Diego, CA) and genotyped for *Bax*. RNA was isolated from $Bax^{+/+}$ ($n = 6$) and $Bax^{-/-}$ ($n = 6$) embryos using the RNeasy Plus Micro Kit (Qiagen) and RNA concentrations were determined with a Qubit Flex Fluorimeter (Thermo Fisher Scientific, Waltham, MA). No more than two embryos of a given genotype were taken from each litter.

2.8 | Whole transcriptome profiling

The UNC High Throughput Sequencing Facility performed RNA sequencing (RNA-seq) using libraries prepared with the SMARTr Ultra Low RNA amp (Clontech, Mountain View, CA) and NexteraXT/NON Stranded kits (Illumina, San Diego, CA). Paired-end (75 bp) sequencing was performed on the Illumina HiSeq 4000. Reads were quality-filtered if at least 90% of bases had a quality score greater than 20 using fastq_quality_filter in FASTX 0.0.14 (http://hannonlab.cshl.edu/fastx_toolkit/index.html).
Adapter sequences were removed using cutadapt 1.12 (Martin, 2011). Reads were then aligned to the mm9 reference genome using STAR 2.5.2b (Dobin et al., 2013). Salmon 0.11.3 (Patro, Duggal, Love, Irizarry, & Kingsford, 2017) with RefSeq gene annotations quantified post-alignment raw counts and RPKM values. One embryo, originally genotyped as $Bax^{-/-}$, had detectable *Bax* mRNA and was not included in the final analysis. Differential expression tests were performed on raw counts using DESeq2 1.22.2 (Anders & Huber, 2010), with significant differences defined by an adjusted p value < .05. The g:profiler toolset (version e104_eg51_p15_3922dba; Raudvere et al., 2019) was used to assess functional enrichment with the following databases: Gene Ontology: Biological Processes, Cellular Component, and Molecular Function; the Kyoto Encyclopedia of Genes and Genomes; Reactome; Corum; Human Phenotype Ontology; and WikiPathways. Additionally, Gene Set Enrichment Analysis (GSEA) Version 7.4 (Mootha et al., 2003; Subramanian et al., 2005) using the Hallmarks and Gene Ontology databases. Cytoscape V3.8.2 (Shannon et al., 2003) was used to visualize the GSEA data and correlations between differentially expressed genes. For examination of chromosome 7, the location of all genes was identified using the Mouse Genome Informatics database (http://www.informatics.jax.org/), and distance from *Bax* was designated as the number of base pairs between the start (3′ end), or terminus (5′ end) of *Bax*, and the nearest end (5′ or 3′) for a particular gene.

3 | RESULTS

3.1 | Fetal dysmorphology

The numbers of $Bax^{+/+}$, $Bax^{+/-}$, and $Bax^{-/-}$ mice followed a closely Mendelian ratio after either of the prenatal treatments (Table 1), confirming that full *Bax* deletion was not lethal. However, alcohol-treated litters were smaller ($t_{59} = 4.0$; $p < .001$) and had more resorptions ($t_{59} = 2.2$; $p = .03$). The maintenance of Mendelian ratios in the alcohol-treated litters indicates that *Bax* deletion did not alter the effects of alcohol on fetal survival. About 14% of vehicle-treated $Bax^{+/+}$ and $Bax^{+/-}$ fetuses had a minor eye defect (Figure 1), primarily on the right side, a rate consistent with our past studies using C57BL/6J mice (Parnell et al., 2006; Parnell et al., 2010). The full *Bax* deletion had a 5% higher incidence of background eye defects (19.1%, $X_1 = 0.19$; $p = .66$), indicating a modest

TABLE 1 Litter characteristics for vehicle and alcohol treatments of *Bax* heterozygous dams

	Litter (n)	Live fetuses	Resorptions	% GT ($^{+/+}$, $^{+/-}$, $^{-/-}$)	n by GT ($^{+/+}$, $^{+/-}$, $^{-/-}$)
Vehicle	28	7.4 ± 0.3	0.11 ± 0.08	27, 50, 23	57, 104, 47
Alcohol	33	**5.7 ± 0.3***	**0.55 ± 0.17***	28, 49, 23	71, 125, 57

Note: Data for live fetuses and resorptions are expressed as the mean litter average (±*SEM*). Emboldened values with asterisks indicate significant differences between vehicle- and alcohol-treated litters ($p < .05$). GT: genotype; $^{+/+}$: wild-type; $^{+/-}$: heterozygous; $^{-/-}$: full knockout.

role of *Bax* in normal eye development. Analysis of lens and globe size in a subset of fetuses revealed that spontaneous defects in the right eyes were very similar between the $Bax^{+/+}$ and $Bax^{-/-}$ fetuses, involving a smaller lens, but a normal-sized globe, and therefore decreases in the ratio of lens to globe size (Figure S1). In contrast, alcohol-induced eye defects tended to be associated with reduced size of both the lens and the globe, and therefore no change in the lens:globe ratio (Figure S1). As observed in C57BL/6J mice, about 50% of alcohol-treated $Bax^{+/+}$ fetuses had an eye defect (53.5%, a 39.5% increase above background; $X_1 = 19.7$; $p < .001$ vs. Vehicle; Figure 1) which ranged in severity from minor decreases in globe size to complete anophthalmia (Table 2). Severe FAS-like facial dysmorphologies occurred in 2/71 wild-type fetuses (2.8%) which included tissue loss in the maxilla corresponding to the lip notch, cleft palate, and disruptions in the vomeronasal organ, as well as the brain

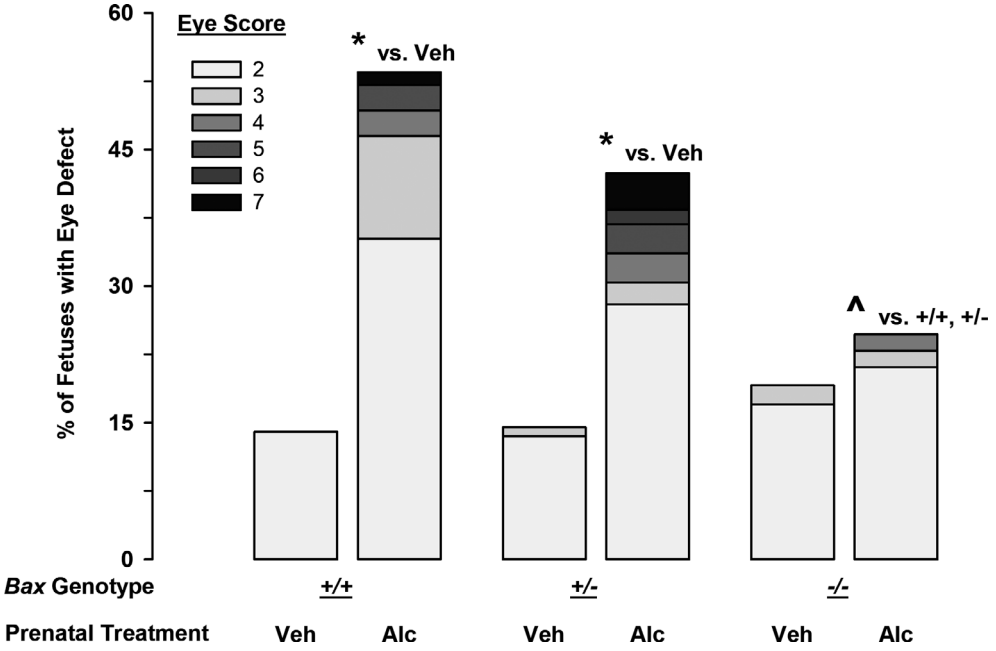

FIGURE 1 Effects of gastrulation-stage alcohol and *Bax* genotype on the incidence and severity of fetal eye defects. Stacked bars portray the percent of fetuses with at least one affected eye in each of the severity categories ranging from 2 (smaller globe or minor change in pupil shape) to 7 (complete anophthalmia) for $Bax^{+/+}$, $Bax^{+/-}$, and $Bax^{-/-}$ fetuses (*left*, *center*, *and right sets of bars*, respectively). The eye score is based on the most severely affected eye for each fetus. * denotes significance versus vehicle-treated fetuses of the same genotype, while the ^ denotes significance versus the alcohol-treated $Bax^{+/+}$ and $Bax^{+/-}$ fetuses ($p < .05$)

TABLE 2 Effects of *Bax* genotype and gastrulation-stage alcohol exposure on the severity of eye defects and incidence of FAS-like facial dysmorphology

	Eye defect severity score							
Drug treatment	**1**	**2**	**3**	**4**	**5**	**6**	**7**	**% FAS-like**
Vehicle								
+/+	49	8	0	0	0	0	0	0
+/−	89	14	1	0	0	0	0	0
−/−	38	8	1	0	0	0	0	0
Alcohol								
+/+	33	25	8	2	2	0	1	2.8%
+/−	72	35	3	4	4	2	5	4%
−/−	43	12	1	1	0	0	0	2%

Note: The data for the most severely affected eye in each fetus are expressed as the number of fetuses with a score from 1 (unaffected) to 7 (anophthalmia). The incidence of non-ocular craniofacial defects is expressed as the percent of fetus with an FAS-like dysmorphology.

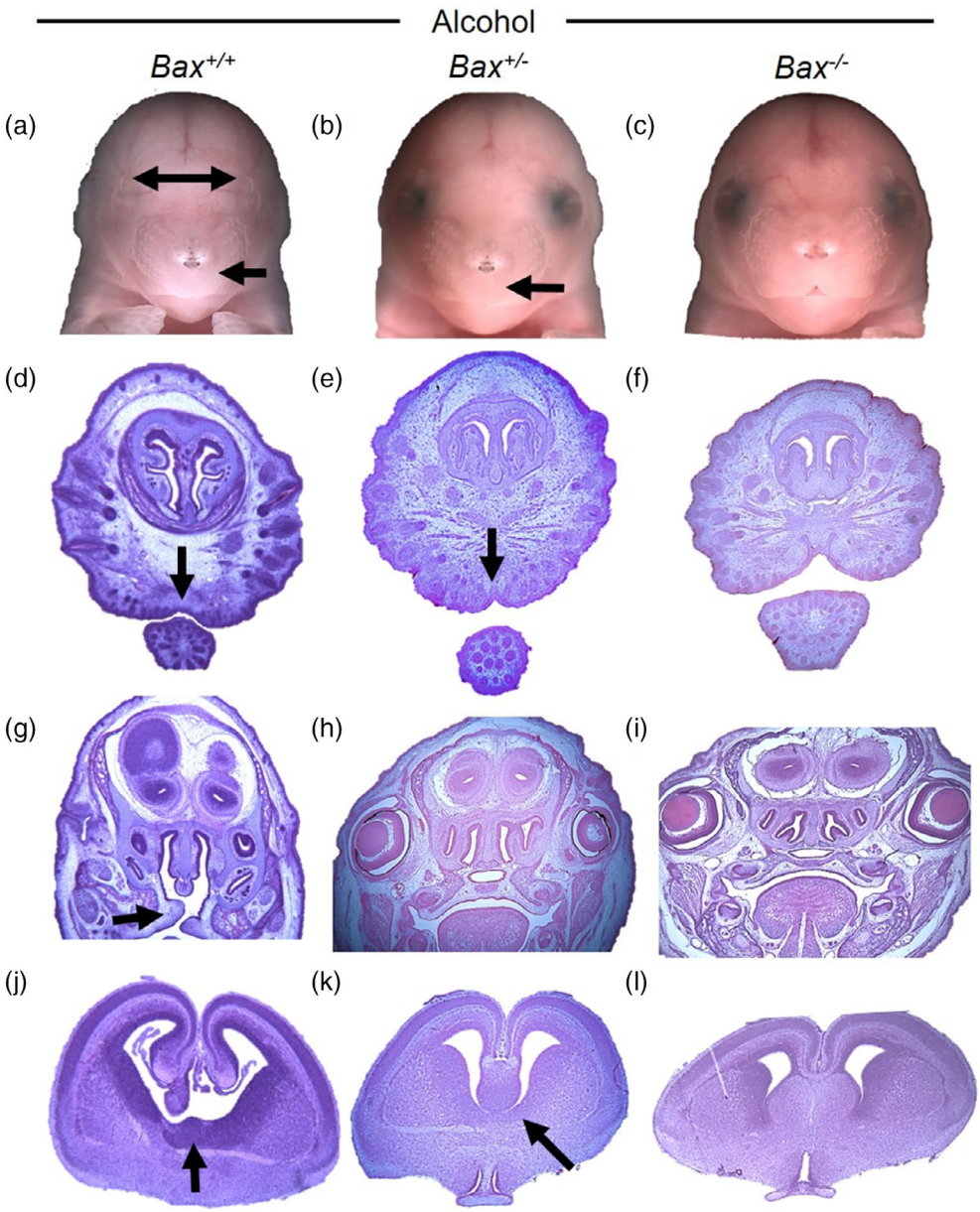

FIGURE 2 Effects of *Bax* genotype on alcohol-induced facial and brain dysmorphology. Photographs of fetal faces (a–c) and of hematoxylin–eosin stained coronal sections through the brain (d–l) are shown for representative $Bax^{+/+}$, $Bax^{+/-}$, and $Bax^{-/-}$ fetuses (*left*, *center*, *and right sets of images*, respectively). Arrows indicate significant dysmorphology including narrowly spaced eye sockets (a), smooth philtrum, absence of lip notch (a, b, d, and e), cleft palate (g), and tissue loss in the brain septal region (j and k). These severe craniofacial effects of alcohol were not observed in the $Bax^{-/-}$ fetuses (c, f, i, and l). Note, colors have been adjusted to minimize differences in hematoxylin–eosin staining intensity

septal area (Figure 2). Holoprosencephaly was also noted in a severely affected fetus (not shown). While partial *Bax* deletion did not significantly modify alcohol-induced eye and craniofacial defects (42.4% had eye defects, a 28% increase above background; $X_1 = 23.3$; $p < .001$ vs. Vehicle; Figure 1, Table 2; 5/125 had FAS-like craniofacial defects [4%]), full *Bax* deletion provided near complete protection from alcohol-induced eye defects (24.6% had eye defects, 5.5% increase from the background incidence, $X_1 = 9.8$; $p = .002$ vs. alcohol-treated $Bax^{+/+}$; $X_1 = 4.6$; $p = .03$ vs. alcohol-treated $Bax^{+/-}$; Figure 1, Table 2) and only 1/57 fetuses (1.8%) had a minor FAS-like facial dysmorphology (i.e., small reduction in the size of the lip notch, with a minor right eye defect; Figure S2). Unfortunately, the small lip notch in the $Bax^{-/-}$ fetus was not identified during the initial dysmorphology exam and the fetus was placed in formalin, which does not provide sufficient drop fixation for the purpose of examining brain sections. Most of the eye defects in $Bax^{+/+}$ fetuses were in the right eye (a 48% vs. a 9% increase from background in the right and left eyes, respectively). A separate analysis of the left and right eyes revealed that the $Bax^{-/-}$ fetuses had significantly fewer right eye defects than did the $Bax^{+/+}$ fetuses, but there was no difference in the left eye (Left, $X_1 = 0.02$; $p = .88$; Right, $X_1 = 8.8$; $p = .003$; Figure S3A). Relatedly, if a $Bax^{+/-}$ or $Bax^{-/-}$ fetus was affected by alcohol, it was more likely to have defects in both the right and left eyes than was a $Bax^{+/+}$ fetus. Among affected mice, the incidence of bilateral eye defects was 13% for $Bax^{+/+}$ fetuses, but 47% and

50% for $Bax^{+/-}$ and $Bax^{-/-}$ fetuses, respectively (Figure S3B). Thus, while deletion of *Bax* provided overall protection from alcohol-induced eye defects, its protective effects were most apparent in the more sensitive right eye.

To examine whether *Bax* deletion affected alcohol-induced apoptosis, embryos were collected and stained with Nile Blue Sulfate (NBS) 12 hr after GD 7 exposure to alcohol or vehicle, a time point corresponding to the highest levels of excessive apoptotic cell death (Kotch & Sulik, 1992). As seen in Figure 3, alcohol-exposed $Bax^{+/+}$ embryos had the highest observable levels of apoptosis, which was localized to the putative ectoderm, consistent with previous findings (Dunty Jr. et al., 2001). The $Bax^{+/-}$ embryos exhibited some apoptosis while little to no apoptosis was observed in the $Bax^{-/-}$ embryos.

3.2 | Differential gene expression in GD 7 $Bax^{-/-}$ embryos

Overall, 63 genes were differentially expressed in the $Bax^{-/-}$ embryos compared with the $Bax^{+/+}$, including 39 down-regulated, and 24 up-regulated genes (Figure 4A, Tables S1 and S2). Examining the chromosomal location of the differentially expressed genes (DEGs) revealed that 31 of the 63 genes (27 down- and four up-regulated) were located on chromosome 7 within relatively close proximity to *Bax* itself (Figure S4; Figure 4B). While most of the DEGs were consistent between individuals of each genotype, one $Bax^{-/-}$ embryo had a pattern of expression for 17 genes that was more similar to the $Bax^{+/+}$ embryos (Figure S5). Examining gene–gene interactions with Cytoscape software, correlations between DEGs were relatively weak, with the strongest correlations between down-regulated genes

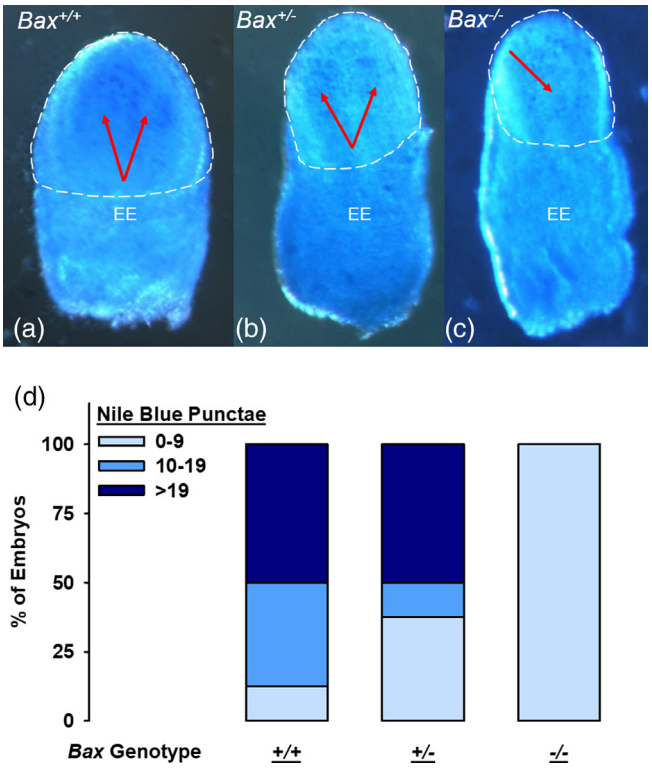

FIGURE 3 Effects of *Bax* genotype on alcohol-induced apoptotic cell death. Panels (a—c) show representative images of the cranial ectoderm side of GD 7 embryos stained with Nile Blue to detect apoptosis. Dashed lines separate the embryo from the extraembryonic tissue (EE). Panel (d) portrays pyknotic cell counts for each of the Bax genotypes: $Bax^{+/+}$ ($n = 8$); $Bax^{+/-}$ ($n = 8$); $Bax^{-/-}$ ($n = 4$), expressed as a % of each genotype with low, moderate, and high levels of cell death

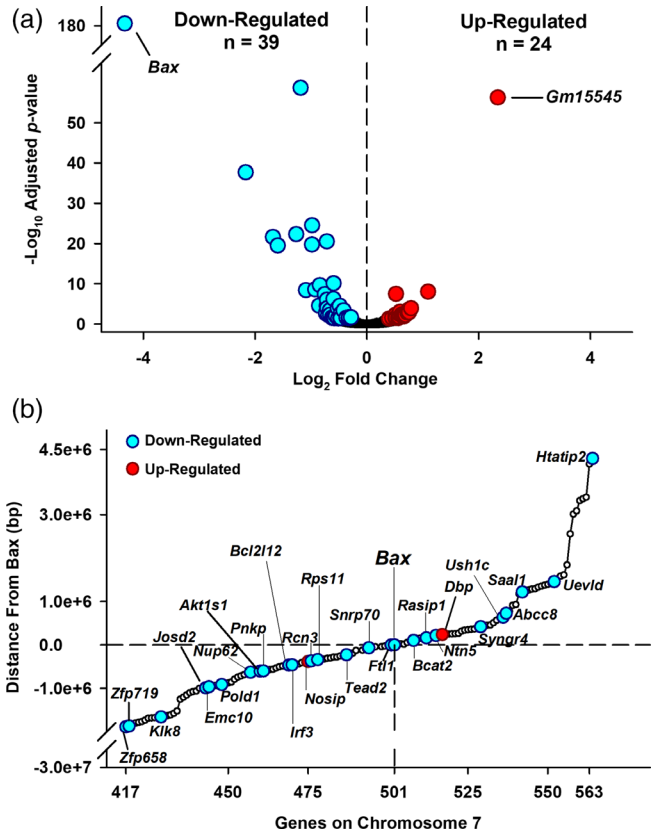

FIGURE 4 Differentially expressed genes in $Bax^{-/-}$ and $Bax^{+/+}$ GD 7 embryos. (a) Volcano plot showing the number of genes significantly downregulated (*cyan circles*) or upregulated (*red circles*) in $Bax^{-/-}$ embryos, as well as genes that were not differentially expressed (*black circles*). (b) Portrayal of differentially expressed genes located on chromosome 7 and their relative proximity (bp) to *Bax*. *Open circles* indicate genes that were located near *Bax*, but were not differentially expressed

observed between *Bcat2* and *Cth*; *Col1a1* and *Rcn3*. The strongest correlations between up-regulated genes existed between *Itga4* and *Itga7*, *Esrrb* and *Nr0b1*, and *Gjb3* and *Gjb5* (Figure S6).

To understand the possible roles of the DEGs, we first examined their function using the published literature (Tables S1, and S2). Most of the DEGs (up-regulated genes are emboldened, down-regulated genes are underlined) were individually associated with key aspects of embryonic/fetal development including: craniofacial/eye/bone development (***Cldn3***, ***Bmp8b***, ***Tmem114***, ***Nosip***, Riox1, Tead2, Ptn, Col1a1, Rgs2, Atoh8, and Pnkp); cell adhesion (***Itgb4***, ***Itga7***, Carmil3, Rasip1, and Ush1c); pluripotency (***Plaur***, Riox1, Saal1, Josd2, Tead2, Ptn, and Akt1s1); and germ cell expression (***Nr0b1***, ***Bmp8b***, ***Esrrb***, and Creb3l4). Many of these genes also have roles in the stimulation of cancer cells (***Itgb4***; ***Plaur***; ***Sycp3***; ***Cldn3***; ***Inpp1***; ***Bcr***; Creb3l4; Josd2; Pold1; Ptn; Col1a1; Pnkp; and Klk8), while others may inhibit cancer cells (***Nlrx1***, Atoh8, Penk, and Htatip2). Several inflammation signaling-related genes were differentially expressed, including: ***Itgb4*** (anti-inflammatory); ***Plaur***; ***Nlrx1***; Pld4; Carmil3; Irf3; and Penk (each are pro-inflammatory). It is noteworthy that, in addition to *Bax*, a large number of genes were associated with either the augmentation (Tead2, Irf3, Rgs2, Penk, and Htatip2), or the inhibition (***Plaur***, ***Ddah1***, ***Bcr***, Riox1, Cth, Creb3l4, Rps11, Pold1, Akt1s1, Pnkp, and Bcl2l12) of apoptosis.

To determine if the DEGs were associated with dysregulation of specific pathways, we first used g:profiler. However, owing to the relatively few DEGs, only 10 pathways were significantly altered, most of which shared similar genes (Figure S7). We next used GSEA which analyzes all genes based on the correlations in their expression and the ranking of genes within a gene set, rather than simply those that are differentially expressed. Thus GSEA is predicted to uncover more potentially dysregulated pathways than g:profiler. The Hallmark pathway analysis revealed that $Bax^{-/-}$ embryos had 27/50 significantly enriched pathways (21 positively- and six negatively enriched pathways) as compared to $Bax^{+/+}$ embryos (Figure S8). It was surprising that there was only a trend (FDR-$p = .085$) toward negative enrichment of apoptotic pathways in the $Bax^{-/-}$ embryos. The absence of a significant negative enrichment may have been because while *Bax* and other genes (*Bgn*, *Cav1*) were ranked lower in the $Bax^{-/-}$ embryos, their core negative enrichment was offset by other genes in this pathway (e.g., *Faslg*, *Gstm1*) that were ranked relatively higher in the $Bax^{-/-}$, but might play a smaller biological role in the control of apoptosis as compared to *Bax* itself. Overall, the Hallmark pathway analysis identified several targets that may uncover the potential interplay between *Bax* and other genes, but functional studies are needed before drawing conclusions on the physiological impact of these enriched gene sets.

A final GSEA examination of the RNAseq data was conducted using the Gene Ontology data set, which includes many more specialized gene sets than does the Hallmark data set. Of the 5,326 reference gene sets, 98 were found to be significantly enriched in either the $Bax^{-/-}$ or $Bax^{+/+}$ embryos. Cytoscape identified that many of these sets could be combined into two large clusters (Figure 5). Positively enriched in the $Bax^{-/-}$ is a large group (25) of cholesterol- and lipid-related sets sharing many of the same genes, with the largest enrichment surrounding *Apoc2* (apolipoprotein C2), one of the top 50-ranked genes. Several small enrichments are found in other apolipoprotein genes, including *Apoa*, *Apoe*, as well as *Pltp* (phospholipid transfer protein). Negatively enriched in the $Bax^{-/-}$ embryos is a large group (18) of ribosomal- and mitochondrial-related gene sets. These sets are enriched due to the effects of a large number of low-ranked genes (e.g., the ribosomal subunit set is enriched in 132/177 genes), rather than a few high-ranked genes, such as *Bax* itself. Examples of such low-ranking genes include the *Mrpls*, *Mrps*, (mammalian mitochondrial ribosomal large and small subunit, respectively), *Malsu* (mitochondrial assembly of ribosomal large subunit 1), *Chchd1* (coiled-coil-helix-coiled-coil-helix domain containing 1), and *Rps11* (ribosomal protein S11). The lipid and ribosomal/mitochondrial clusters illustrate the advantage of GSEA over analyses that only include DEGs, in that two key cellular functions are identified that would not have been predicted using DEGs alone.

In addition, 40 other gene sets were positively enriched in the $Bax^{-/-}$ embryos (Table S3), with general functions related to apoptosis, placental development, coagulation, cellular membrane and permeability, gene expression or replication, receptor binding and channel activity, organelles, and other processes. Interestingly, positive enrichment was found in gene sets related to hydrogen peroxide and reactive oxygen species (ROS). Eleven gene sets not related to ribosomes and mitochondria were found to be negatively enriched in the $Bax^{-/-}$ embryos (Table S4), related to the general functions of apoptosis, organelles, somite development, and remodeling. *Bax* itself was associated with all of these pathways, with the exception of somitogenesis and somite development.

4 | DISCUSSION

Alcohol exposure during the developmental stage of gastrulation triggers interacting pathogenic cascades that

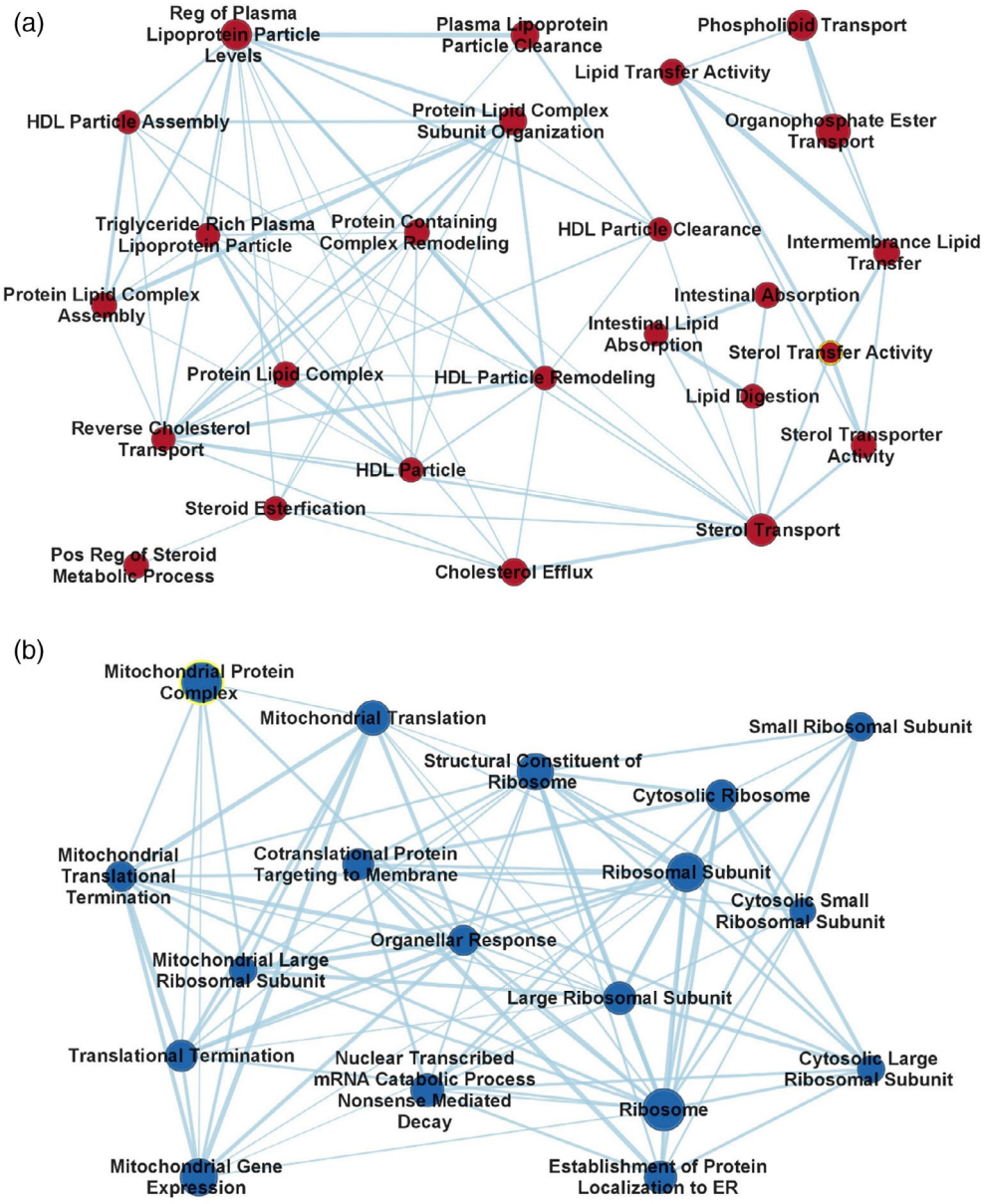

FIGURE 5 Clustering of significantly enriched pathways in *Bax*$^{-/-}$ embryos identified in GSEA Gene Ontology. (a) Relationships between positively enriched gene sets related to lipid membranes and cholesterol. (b) Relationships between negatively enriched gene sets related to mitochondria. Mitochondrial protein complex is highlighted in yellow because it is the only pathway in which *Bax* contributed significant enrichment. Symbol size reflects the number of genes in each set

cause the craniofacial and brain dysmorphologies characteristic of FAS. Excessive ectodermal cell death was the first described pathogenic mechanism (Sulik, Johnston, & Webb, 1981) and more recent research has uncovered the cellular events that orchestrate the transition from developmentally appropriate cell death to the excessive cell death that ultimately compromises the fetus. The present results uphold the role of apoptotic death in the expression of gastrulation stage alcohol-induced craniofacial dysmorphologies, and importantly, highlight the critical, pernicious role of Bax. Full deletion of the *Bax* gene reduced the incidence of alcohol-induced eye, face, and brain defects, while also minimizing cell death following the alcohol exposure. Other than *Bax* itself, a relatively small number of genes were differentially expressed between untreated *Bax*$^{+/+}$ and *Bax*$^{-/-}$ embryos and these genes may reflect the direct consequences of *Bax* deletion or compensatory mechanisms that enable the typical development of *Bax*$^{-/-}$ embryos. In addition to the DEGs, the GSEA analysis revealed more global changes in gene expression and highlighted several biological functions beyond apoptosis that may be affected by *Bax* deletion.

The craniofacial and brain dysmorphologies observed in the *Bax*$^{+/+}$ and *Bax*$^{+/-}$ fetuses are consistent in incidence and severity with those previously observed in mice on the C57BL/6J background (Dou et al., 2013; Godin et al., 2010). The most frequent defects observed in the *Bax*$^{+/+}$ and *Bax*$^{+/-}$ fetuses were varying degrees of microphthalmia, a common occurrence in children with FASD (Del Campo & Jones, 2017). Some fetuses were severely affected, demonstrating complete anophthalmia,

facial dysmorphologies, and holoprosencephaly, consistent with the idea that FAS falls into the holoprosencephaly spectrum (Hong & Krauss, 2012, 2017; Lipinski et al., 2010; Sulik, 1984). At first glance, these severe dysmorphologies might be surprising given the relatively sparse ectodermal cell death detected by the Nile Blue staining. However, the amount and pattern of staining in the $Bax^{+/+}$ and $Bax^{+/-}$ embryos was similar to that observed previously in C57BL/6J mice (Dunty Jr. et al., 2001). While Nile Blue is rapid and allows post-processing genotyping, it captures only a snap-shot of the total embryonic cell death (Sulik, Cook, & Webster, 1988), which may persist beyond the currently studied time window. At the mid- to late-gastrulation stages measured herein, prior to optic evagination, the ectodermal cell death observed here demonstrates death in the cells that give rise to the forebrain and eyes. Most importantly, apoptotic cell death was attenuated in the $Bax^{-/-}$ embryos, mice whose craniofacies were largely unaffected by a gastrulation-stage alcohol exposure. The very slight protection provided by the $Bax^{+/-}$ genotype on embryonic cell death and the presence of particularly severe facial dysmorphologies in the $Bax^{+/-}$ fetuses do not provide convincing evidence for a gene-dose effect, but instead support the hypothesis that an all-or-none threshold of Bax is required for gastrulation alcohol-induced dysmorphologies, as also demonstrated for retinal damage (Semaan et al., 2010). That $Bax^{-/-}$ was not fully protective against alcohol-induced dysmorphologies (alcohol caused a small increase in the incidence of eye defects and one $Bax^{-/-}$ had a relatively minor FAS-like facial defect) suggests the involvement of other, Bax-independent, mechanisms of teratogenesis. One possibility is a partial substitution by Bak in the induction of mitochondrial cell death, or the involvement of the extrinsic cell death pathway, the activity of which is unaffected by *Bax* deletion (Mac Nair et al., 2016).

Previous research on the importance of Bax in FASD models has focused on third trimester-equivalent exposure which causes large amounts of neuronal cell death in the cerebellum and regions of the cortex (Ahlers, Karacay, Fuller, Bonthius, & Dailey, 2015; Britton & Miller, 2018; Heaton et al., 2006; Heaton, Paiva, & Kubovec, 2015; Young et al., 2003). The extension of Bax's apoptotic role to the gastrulation-stage embryo raises the question as to whether particular cell phenotypes are spared or remain sensitive to alcohol-induced cell death. Prior studies have shown that Bax affects survival of post-mitotic neurons, and not the neuronal progenitor cells (D'Sa-Eipper et al., 2001; Jung et al., 2008; Lindsten et al., 2000; Shi, Parada, & Kernie, 2005), but it is unclear whether a similar distinction occurs during gastrulation, prior to neurogenesis. Not all cells at gastrulation will have progressed enough to develop the capacity for apoptosis, and it is possible that these may become sensitive only during a second wave of apoptosis (Cartwright, Tessmer, & Smith, 1998; Olney et al., 2002; Young et al., 2003). Nonetheless, there is now converging evidence that Bax is necessary for alcohol-induced apoptosis at different times in development and is therefore critical to many different FASD outcomes. While we report a role for Bax in craniofacial dysmorphology, which is associated with major tissue loss, future studies should examine other, more subtle, sequelae of gastrulation-stage PAE, such as hypothalamic–pituitary–adrenal axis activity and behavioral alterations (Wieczorek, Fish, O'Leary-Moore, Parnell, & Sulik, 2015), to uncover the full contribution of Bax.

The current results suggest that the accumulation of Bax in the mitochondrial membrane is the decisive event determining a cell's fate after PAE and ultimately whether an individual develops, or is shielded from, an FAS-like dysmorphology. However, a tapestry of cellular signals must interact before this fate is decided and acute alcohol has been shown to affect many of these interactions. First, acute PAE may initiate cell death machinery by inducing metabolic stress, restricting blood flow, and affecting cell adhesion. Previous studies have shown that PAE can activate Tp53 signaling, one of the signals that begin the apoptotic cascade (Anthony, Zhou, Ogawa, Goodlett, & Ruiz, 2008; Flentke, Baulch, Berres, Garic, & Smith, 2019; Ignacio, Mooney, & Middleton, 2014; Kuhn & Miller, 1998), and that genetic deletion of *Tp53* is also protective from PAE (Fish, Tucker, Peterson, Eberhart, & Parnell, 2021). Once Tp53, or other signals, initiate the apoptotic cascade, changes in the expression and activity of the BH3 protein family have the dual role to inhibit the pro-survival Bcl-2 signals, which normally keep Bax in check, and directly activate Bax itself. In a transcriptome-wide study, gastrulation-stage PAE upregulated one of these BH3 signals, *Bid* (Boschen, Ptacek, et al., 2021), which is also activated by caspase-8 through the extrinsic pathway and is increased following postnatal alcohol exposure (Heaton et al., 2015). Repeated PAE impairs Bcl-2 protein expression (Mooney & Miller, 2001), which may be sufficient to allow Bax to accumulate in the mitochondrial membrane and induce cell death. Taken together, these data strongly support a model where PAE converges on multiple apoptotic mechanisms within the intrinsic cell death pathway, of which Bax is the final arbiter.

We performed whole transcriptomic RNA sequencing to identify genes significantly altered by the *Bax* deletion, prior to alcohol exposure. While it would have been ideal to focus on a discrete subtype of embryonic cells, such as the ectoderm, using the whole embryo provided more

consistent sequencing results. This analysis provided information regarding other genes throughout the embryo that were modified by the *Bax* deletion and could, like *Bax*, affect the sensitivity to PAE and provide both alternative interpretations to our results, as well as identify future targets of study. Only 63 genes were differentially expressed between untreated $Bax^{+/+}$ and $Bax^{-/-}$ GD 7 embryos. Nearly half of the DEGs were found on chromosome 7, in proximity to *Bax*, suggesting that these are directly due to the insertion of the neo-cassette used to generate the $Bax^{-/-}$ mice (Meier et al., 2010; Pham, MacIvor, Hug, Heusel, & Ley, 1996; Sato et al., 2000; West et al., 2016). None of the DEGs was as dysregulated as *Bax* itself and several of the up-regulated genes, in particular, were expressed at low levels, raising questions of their functional impact. Moreover, there was variation between individuals, suggesting that the alternate gene expression is not a definite consequence of the *Bax* deletion.

Functional profiling of the up/down-regulated DEGs using g:profiler was limited by the relatively small number of input genes. However, GSEA, which examines the interaction between all expressed genes, identified multiple pathways that were differentially enriched in the $Bax^{+/+}$ and $Bax^{-/-}$ embryos (see Figures S7 and S8, and Tables S3 and S4). Since significant enrichment of a gene does not distinguish functional up- or down-regulation, the gene clusters identified by GSEA serve mainly as rationale for future studies. Two large clusters were identified by the Gene Ontology database: a negatively enriched mitochondria-related set; and a positively enriched lipid-related set. Bax and Bak play a non-apoptotic role in mitochondrial dynamics; *Bax* deletion shortens mitochondria and reduces rates of fusion (Hoppins et al., 2011; Karbowski, Norris, Cleland, Jeong, & Youle, 2006). An alternative explanation about the critical effect of the *Bax* deletion could be a background shift in the mitochondrial dynamics of $Bax^{-/-}$ embryos, which might render them less sensitive to the effects of the existing pro-apoptotic proteins Bak and Bid. The viability of this hypothesis remains to be tested. Overall, the negative enrichment of the mitochondrial-related gene set in the $Bax^{-/-}$ embryos spotlights the potential of future studies on the role of mitochondria during gastrulation-stage alcohol exposure.

Apolipoproteins and cholesterol are essential for the development and maintenance of cellular membranes; inhibition of these lipids is associated with embryonic cell death and craniofacial malformations (Homanics et al., 1995; Lanoue et al., 1997). $Bax^{-/-}$ embryos were positively enriched in genes related to cholesterol and lipids and it is possible that these may also promote further resistance to the effects of alcohol. Although gastrulation-stage PAE did not affect gene expression of apolipoproteins in the C57BL/6J or C57BL/6NHsd strains (Boschen, Ptacek, et al., 2021), alcohol has long been shown to disrupt lipid membranes (Goldstein, 1984; Klemm, 1998; Patra et al., 2006) and this disruption could be a signal that triggers the apoptotic cascade. Moreover, cholesterol and apolipoproteins are critical to the synthesis and packaging of Sonic hedgehog (Shh; Briscoe & Therond, 2013). Since gastrulation-stage alcohol exposure strongly inhibits Shh signaling (Ahlgren et al., 2002; Boschen, Fish, & Parnell, 2021; Hong & Krauss, 2012; Kahn et al., 2017; Zhang et al., 2013), and this inhibition is necessary for craniofacial dysmorphology, examining the interaction between Bax and Shh signaling is a logical extension of the current study. Additionally, positive enrichment in apolipoproteins may further account for the later life enhancement of oligodendrocyte density and axonal density in $Bax^{-/-}$ brains (Kawai et al., 2009; White et al., 1998) and changes in $Bax^{-/-}$ retina (Kawai et al., 2009; Mac Nair et al., 2016; Mosinger Ogilvie et al., 1998).

A critical question is whether the DEGs and/or the enriched pathways influence the protective effect of *Bax* deletion on alcohol-induced dysmorphologies. Current experiments are underway employing an *Irf3-Bcl2l12* mouse mutant, but *Htatip2*, *Cth*, *Plaur*, *Riox1*, *Creb3l4*, *Akt1s1*, and *Pnkp* are all sensitive to early PAE in the C57BL/6J mouse strain (Boschen, Ptacek, et al., 2021; Boschen and Parnell, unpublished observations) and their identity as potential mediators of alcohol teratogenesis should also be examined. Additionally, two DEGs, *Ddah1* and *Nosip*, warrant continued investigation since prior studies show a protective role for nitric oxide in FASDs (Bonthius et al., 2002; Karacay & Bonthius, 2015). The potential importance of ROS is supported by the GSEA finding of positive enrichment of genes related to hydrogen peroxide and ROS biosynthetic processes, both of which have roles for *Duox2* (dual oxidase maturation factor 2).

In summary, the experiments described herein find a pathogenic role for Bax during gastrulation-stage alcohol exposure. Attenuation of alcohol-induced apoptosis is a mechanism through which *Bax* gene deletion protects the embryo, but changes in the expression of genes other than *Bax* reveal that *Bax* deletion potentially affects other aspects of embryonic physiology. Whether these changes are relevant to the protective effects of *Bax* deletion on craniofacial dysmorphology can be addressed by future studies using acute pharmacological inhibitors of Bax (Jensen, WuWong, Wong, Matsuyama, & Matsuyama, 2019), which may help pin-point the critical timing of Bax's deleterious effects on the embryo. Importantly, *Bax* may be a key gene that modifies susceptibilities to FASD.

Several *Bax* single nucleotide polymorphisms have been linked to cancer risk and treatment response (Peng et al., 2015; Saxena, Moshynska, Sankaran, Viswanathan, & Sheridan, 2002; L. Sun, Wei, Wei, & Li, 2018) and *Bax* loss of function variants, while elevating risk for cancers, may reduce the risk for at least some FASD symptoms, especially those, like craniofacial malformations, that are caused by apoptotic cell death.

ACKNOWLEDGMENTS

The authors appreciate the assistance of Lorinda K. Baker and Laura B. Murdaugh for their initial maintenance of the *Bax* colony and Rachel L. Peterson for photography of formalin-fixed fetuses. We also thank Melina Steensen and Casey Hunter for performing the specimen sectioning and histological staining. This research was supported by U01-AA021651 from the National Institute on Alcohol Abuse and Alcoholism (NIAAA) to SEP. All or part of this work was done in conjunction with the Collaborative Initiative on Fetal Alcohol Spectrum Disorders (CIFASD), which is funded by grants from the NIAAA. Additional information about CIFASD can be found at www.cifasd.org. AH and JMS are supported by U54-HD079124 from the Eunice Kennedy Shriver National Institute of Child Health and Human Development (NICHD), and P30NS045892 from the National Institute of Neurological Disorders and Stroke (NINDS).

CONFLICT OF INTEREST

The authors declare no conflicts of interest.

DATA AVAILABILITY STATEMENT

The data that support the findings of this study are available from the corresponding author upon reasonable request.

ORCID

Eric W. Fish https://orcid.org/0000-0001-6598-5654
Haley N. Mendoza-Romero https://orcid.org/0000-0001-7290-9246

REFERENCES

Abel, E. L. (1995). An update on incidence of Fas—Fas is not an equal-opportunity birth-defect. *Neurotoxicology and Teratology*, *17*(4), 437–443. https://doi.org/10.1016/0892-0362(95)00005-C

Ahlers, K. E., Karacay, B., Fuller, L., Bonthius, D. J., & Dailey, M. E. (2015). Transient activation of microglia following acute alcohol exposure in developing mouse neocortex is primarily driven by BAX-dependent neurodegeneration. *Glia*, *63*(10), 1694–1713. https://doi.org/10.1002/glia.22835

Ahlgren, S. C., Thakur, V., & Bronner-Fraser, M. (2002). Sonic hedgehog rescues cranial neural crest from cell death induced by ethanol exposure. *Proceedings of the National Academy of Sciences of the United States of America*, *99*(16), 10476–10481. https://doi.org/10.1073/pnas.162356199

Anders, S., & Huber, W. (2010). Differential expression analysis for sequence count data. *Genome Biology*, *11*(10), R106. https://doi.org/10.1186/gb-2010-11-10-r106

Anthony, B., Zhou, F. C., Ogawa, T., Goodlett, C. R., & Ruiz, J. (2008). Alcohol exposure alters cell cycle and apoptotic events during early neurulation. *Alcohol and Alcoholism*, *43*(3), 261–273. https://doi.org/10.1093/alcalc/agm166

Bonthius, D. J., Tzouras, G., Karacay, B., Mahoney, J., Hutton, A., McKim, R., & Pantazis, N. J. (2002). Deficiency of neuronal nitric oxide synthase (nNOS) worsens alcohol-induced microencephaly and neuronal loss in developing mice. *Brain Research. Developmental Brain Research*, *138*(1), 45–59. https://doi.org/10.1016/s0165-3806(02)00458-3

Boschen, K. E., Fish, E. W., & Parnell, S. E. (2021). Prenatal alcohol exposure disrupts sonic hedgehog pathway and primary cilia genes in the mouse neural tube. *Reproductive Toxicology*, *105*, 136–147. https://doi.org/10.1016/j.reprotox.2021.09.002

Boschen, K. E., Ptacek, T. S., Berginski, M. E., Simon, J. M., & Parnell, S. E. (2021). Transcriptomic analyses of gastrulation-stage mouse embryos with differential susceptibility to alcohol. *Disease Models & Mechanisms*, *14*(6). https://doi.org/10.1242/dmm.049012

Briscoe, J., & Therond, P. P. (2013). The mechanisms of hedgehog signalling and its roles in development and disease. *Nature Reviews. Molecular Cell Biology*, *14*(7), 416–429. https://doi.org/10.1038/nrm3598

Britton, S. M., & Miller, M. W. (2018). Neuronal loss in the developing cerebral cortex of Normal and Bax-deficient mice: Effects of ethanol exposure. *Neuroscience*, *369*, 278–291. https://doi.org/10.1016/j.neuroscience.2017.11.013

Cartwright, M. M., Tessmer, L. L., & Smith, S. M. (1998). Ethanol-induced neural crest apoptosis is coincident with their endogenous death, but is mechanistically distinct. *Alcoholism, Clinical and Experimental Research*, *22*(1), 142–149.

Deckwerth, T. L., Elliott, J. L., Knudson, C. M., Johnson, E. M., Jr., Snider, W. D., & Korsmeyer, S. J. (1996). BAX is required for neuronal death after trophic factor deprivation and during development. *Neuron*, *17*(3), 401–411. https://doi.org/10.1016/s0896-6273(00)80173-7

Del Campo, M., & Jones, K. L. (2017). A review of the physical features of the fetal alcohol spectrum disorders. *European Journal of Medical Genetics*, *60*(1), 55–64. https://doi.org/10.1016/j.ejmg.2016.10.004

Dobin, A., Davis, C. A., Schlesinger, F., Drenkow, J., Zaleski, C., Jha, S., ... Gingeras, T. R. (2013). STAR: ultrafast universal RNA-seq aligner. *Bioinformatics*, *29*(1), 15–21. https://doi.org/10.1093/bioinformatics/bts635

Dou, X., Wilkemeyer, M. F., Menkari, C. E., Parnell, S. E., Sulik, K. K., & Charness, M. E. (2013). Mitogen-activated protein kinase modulates ethanol inhibition of cell adhesion mediated by the L1 neural cell adhesion molecule. *Proceedings of the National Academy of Sciences of the United States of America*, *110*(14), 5683–5688. https://doi.org/10.1073/pnas.1221386110

D'Sa-Eipper, C., Leonard, J. R., Putcha, G., Zheng, T. S., Flavell, R. A., Rakic, P., ... Roth, K. A. (2001). DNA damage-induced neural precursor cell apoptosis requires p53 and caspase 9 but neither Bax nor caspase 3. *Development*, *128*(1), 137–146.

Dunty, W. C., Jr., Chen, S. Y., Zucker, R. M., Dehart, D. B., & Sulik, K. K. (2001). Selective vulnerability of embryonic cell

populations to ethanol-induced apoptosis: Implications for alcohol-related birth defects and neurodevelopmental disorder. *Alcoholism, Clinical and Experimental Research*, *25*(10), 1523–1535.

Eberhart, J. K., & Parnell, S. E. (2016). The genetics of fetal alcohol Spectrum disorders. *Alcoholism, Clinical and Experimental Research*, *40*(6), 1154–1165. https://doi.org/10.1111/acer.13066

Fish, E. W., Tucker, S. K., Peterson, R. L., Eberhart, J. K., & Parnell, S. E. (2021). Loss of tumor protein 53 protects against alcohol-induced facial malformations in mice and zebrafish. *Alcoholism, Clinical and Experimental Research*, *45*, 1965–1979. https://doi.org/10.1111/acer.14688

Flentke, G. R., Baulch, J. W., Berres, M. E., Garic, A., & Smith, S. M. (2019). Alcohol-mediated calcium signals dysregulate pro-survival Snai2/PUMA/Bcl2 networks to promote p53-mediated apoptosis in avian neural crest progenitors. *Birth Defects Research*, *111*(12), 686–699. https://doi.org/10.1002/bdr2.1508

Forger, D. B., & Peskin, C. S. (2005). Stochastic simulation of the mammalian circadian clock. *Proceedings of the National Academy of Sciences of the United States of America*, *102*(2), 321–324. https://doi.org/10.1073/pnas.0408465102

Gilbert, M. T., Sulik, K. K., Fish, E. W., Baker, L. K., Dehart, D. B., & Parnell, S. E. (2016). Dose-dependent teratogenicity of the synthetic cannabinoid CP-55,940 in mice. *Neurotoxicology and Teratology*, *58*, 15–22. https://doi.org/10.1016/j.ntt.2015.12.004

Godin, E. A., O'Leary-Moore, S. K., Khan, A. A., Parnell, S. E., Ament, J. J., Dehart, D. B., ... Sulik, K. K. (2010). Magnetic resonance microscopy defines ethanol-induced brain abnormalities in prenatal mice: Effects of acute insult on gestational day 7. *Alcoholism, Clinical and Experimental Research*, *34*(1), 98–111. https://doi.org/10.1111/j.1530-0277.2009.01071.x

Goldstein, D. B. (1984). The effects of drugs on membrane fluidity. *Annual Review of Pharmacology and Toxicology*, *24*, 43–64. https://doi.org/10.1146/annurev.pa.24.040184.000355

Heaton, M. B., Paiva, M., & Kubovec, S. (2015). Differential effects of ethanol on bid, tBid, and Bax:tBid interactions in postnatal day 4 and postnatal day 7 rat cerebellum. *Alcoholism, Clinical and Experimental Research*, *39*(1), 55–63. https://doi.org/10.1111/acer.12603

Heaton, M. B., Paiva, M., Madorsky, I., Siler-Marsiglio, K., & Shaw, G. (2006). Effect of bax deletion on ethanol sensitivity in the neonatal rat cerebellum. *Journal of Neurobiology*, *66*(1), 95–101. https://doi.org/10.1002/neu.20208

Homanics, G. E., Maeda, N., Traber, M. G., Kayden, H. J., Dehart, D. B., & Sulik, K. K. (1995). Exencephaly and hydrocephaly in mice with targeted modification of the apolipoprotein B (Apob) gene. *Teratology*, *51*(1), 1–10. https://doi.org/10.1002/tera.1420510102

Hong, M., & Krauss, R. S. (2012). Cdon mutation and fetal ethanol exposure synergize to produce midline signaling defects and holoprosencephaly spectrum disorders in mice. *PLoS Genetics*, *8*(10), e1002999. https://doi.org/10.1371/journal.pgen.1002999

Hong, M., & Krauss, R. S. (2017). Ethanol itself is a holoprosencephaly-inducing teratogen. *PLoS One*, *12*(4), e0176440. https://doi.org/10.1371/journal.pone.0176440

Hoppins, S., Edlich, F., Cleland, M. M., Banerjee, S., McCaffery, J. M., Youle, R. J., & Nunnari, J. (2011). The soluble form of Bax regulates mitochondrial fusion via MFN2 homotypic complexes. *Molecular Cell*, *41*(2), 150–160. https://doi.org/10.1016/j.molcel.2010.11.030

Ignacio, C., Mooney, S. M., & Middleton, F. A. (2014). Effects of acute prenatal exposure to ethanol on microRNA expression are ameliorated by social enrichment. *Frontiers in Pediatrics*, *2*, 103. https://doi.org/10.3389/fped.2014.00103

Jensen, K., WuWong, D. J., Wong, S., Matsuyama, M., & Matsuyama, S. (2019). Pharmacological inhibition of Bax-induced cell death: Bax-inhibiting peptides and small compounds inhibiting Bax. *Experimental Biology and Medicine*, *244*(8), 621–629. https://doi.org/10.1177/1535370219833624

Jung, A. R., Kim, T. W., Rhyu, I. J., Kim, H., Lee, Y. D., Vinsant, S., ... Sun, W. (2008). Misplacement of Purkinje cells during postnatal development in Bax knock-out mice: A novel role for programmed cell death in the nervous system? *The Journal of Neuroscience: The Official Journal of the Society for Neuroscience*, *28*(11), 2941–2948. https://doi.org/10.1523/JNEUROSCI.3897-07.2008

Kahn, B. M., Corman, T. S., Lovelace, K., Hong, M., Krauss, R. S., & Epstein, D. J. (2017). Prenatal ethanol exposure in mice phenocopies Cdon mutation by impeding Shh function in the etiology of optic nerve hypoplasia. *Disease Models & Mechanisms*, *10*(1), 29–37. https://doi.org/10.1242/dmm.026195

Karacay, B., & Bonthius, D. J. (2015). The neuronal nitric oxide synthase (nNOS) gene and neuroprotection against alcohol toxicity. *Cellular and Molecular Neurobiology*, *35*(4), 449–461. https://doi.org/10.1007/s10571-015-0155-0

Karbowski, M., Norris, K. L., Cleland, M. M., Jeong, S. Y., & Youle, R. J. (2006). Role of Bax and Bak in mitochondrial morphogenesis. *Nature*, *443*(7112), 658–662. https://doi.org/10.1038/nature05111

Kawai, K., Itoh, T., Itoh, A., Horiuchi, M., Wakayama, K., Bannerman, P., ... Lindsten, T. (2009). Maintenance of the relative proportion of oligodendrocytes to axons even in the absence of BAX and BAK. *The European Journal of Neuroscience*, *30*(11), 2030–2041. https://doi.org/10.1111/j.1460-9568.2009.06988.x

Kelly, S. J., Day, N., & Streissguth, A. P. (2000). Effects of prenatal alcohol exposure on social behavior in humans and other species. *Neurotoxicology and Teratology*, *22*(2), 143–149.

Klemm, W. R. (1998). Biological water and its role in the effects of alcohol. *Alcohol*, *15*(3), 249–267. https://doi.org/10.1016/s0741-8329(97)00130-4

Knudson, C. M., Tung, K. S., Tourtellotte, W. G., Brown, G. A., & Korsmeyer, S. J. (1995). Bax-deficient mice with lymphoid hyperplasia and male germ cell death. *Science*, *270*(5233), 96–99. https://doi.org/10.1126/science.270.5233.96

Kotch, L. E., & Sulik, K. K. (1992). Patterns of ethanol-induced cell death in the developing nervous system of mice; neural fold states through the time of anterior neural tube closure. *International Journal of Developmental Neuroscience*, *10*(4), 273–279.

Kuhn, P. E., & Miller, M. W. (1998). Expression of p53 and ALZ-50 immunoreactivity in rat cortex: Effect of prenatal exposure to ethanol. *Experimental Neurology*, *154*(2), 418–429. https://doi.org/10.1006/exnr.1998.6907

Lanoue, L., Dehart, D. B., Hinsdale, M. E., Maeda, N., Tint, G. S., & Sulik, K. K. (1997). Limb, genital, CNS, and facial malformations result from gene/environment-induced cholesterol

deficiency: Further evidence for a link to sonic hedgehog. *American Journal of Medical Genetics*, *73*(1), 24–31.

Lindsten, T., Ross, A. J., King, A., Zong, W. X., Rathmell, J. C., Shiels, H. A., ... Thompson, C. B. (2000). The combined functions of proapoptotic Bcl-2 family members bak and bax are essential for normal development of multiple tissues. *Molecular Cell*, *6*(6), 1389–1399. https://doi.org/10.1016/s1097-2765(00)00136-2

Lipinski, R. J., Song, C., Sulik, K. K., Everson, J. L., Gipp, J. J., Yan, D., ... Rowland, I. J. (2010). Cleft lip and palate results from hedgehog signaling antagonism in the mouse: Phenotypic characterization and clinical implications. *Birth Defects Research. Part A, Clinical and Molecular Teratology*, *88*(4), 232–240. https://doi.org/10.1002/bdra.20656

Mac Nair, C. E., Schlamp, C. L., Montgomery, A. D., Shestopalov, V. I., & Nickells, R. W. (2016). Retinal glial responses to optic nerve crush are attenuated in Bax-deficient mice and modulated by purinergic signaling pathways. *Journal of Neuroinflammation*, *13*(1), 93. https://doi.org/10.1186/s12974-016-0558-y

Martin, M. (2011). Cutadapt removes adapter sequences from high-throughput sequencing reads. *EMBnet. Journal*, *17*, 10–12.

Mattson, S. N., Crocker, N., & Nguyen, T. T. (2011). Fetal alcohol spectrum disorders: Neuropsychological and behavioral features. *Neuropsychology Review*, *21*(2), 81–101. https://doi.org/10.1007/s11065-011-9167-9

May, P. A., Chambers, C. D., Kalberg, W. O., Zellner, J., Feldman, H., Buckley, D., ... Hoyme, H. E. (2018). Prevalence of fetal alcohol Spectrum disorders in 4 US communities. *JAMA*, *319*(5), 474–482. https://doi.org/10.1001/jama.2017.21896

Meier, I. D., Bernreuther, C., Tilling, T., Neidhardt, J., Wong, Y. W., Schulze, C., ... Schachner, M. (2010). Short DNA sequences inserted for gene targeting can accidentally interfere with off-target gene expression. *FASEB Journal: Official Publication of the Federation of American Societies for Experimental Biology*, *24*(6), 1714–1724. https://doi.org/10.1096/fj.09-140749

Mooney, S. M., & Miller, M. W. (2001). Effects of prenatal exposure to ethanol on the expression of bcl-2, bax and caspase 3 in the developing rat cerebral cortex and thalamus. *Brain Research*, *911*(1), 71–81. https://doi.org/10.1016/s0006-8993(01)02718-4

Mootha, V. K., Lindgren, C. M., Eriksson, K. F., Subramanian, A., Sihag, S., Lehar, J., ... Groop, L. C. (2003). PGC-1alpha-responsive genes involved in oxidative phosphorylation are coordinately downregulated in human diabetes. *Nature Genetics*, *34*(3), 267–273. https://doi.org/10.1038/ng1180

Mosinger Ogilvie, J., Deckwerth, T. L., Knudson, C. M., & Korsmeyer, S. J. (1998). Suppression of developmental retinal cell death but not of photoreceptor degeneration in Bax-deficient mice. *Investigative Ophthalmology & Visual Science*, *39*(9), 1713–1720.

Olney, J. W., Tenkova, T., Dikranian, K., Muglia, L. J., Jermakowicz, W. J., D'Sa, C., & Roth, K. A. (2002). Ethanol-induced caspase-3 activation in the in vivo developing mouse brain. *Neurobiology of Disease*, *9*(2), 205–219. https://doi.org/10.1006/nbdi.2001.0475

Parnell, S. E., Dehart, D. B., Wills, T. A., Chen, S. Y., Hodge, C. W., Besheer, J., ... Sulik, K. K. (2006). Maternal oral intake mouse model for fetal alcohol spectrum disorders: Ocular defects as a measure of effect. *Alcoholism, Clinical and Experimental Research*, *30*(10), 1791–1798. https://doi.org/10.1111/j.1530-0277.2006.00212.x

Parnell, S. E., Sulik, K. K., Dehart, D. B., & Chen, S. Y. (2010). Reduction of ethanol-induced ocular abnormalities in mice through dietary administration of N-acetylcysteine. *Alcohol*, *44*(7–8), 699–705. https://doi.org/10.1016/j.alcohol.2010.05.006

Patra, M., Salonen, E., Terama, E., Vattulainen, I., Faller, R., Lee, B. W., ... Karttunen, M. (2006). Under the influence of alcohol: The effect of ethanol and methanol on lipid bilayers. *Biophysical Journal*, *90*(4), 1121–1135. https://doi.org/10.1529/biophysj.105.062364

Patro, R., Duggal, G., Love, M. I., Irizarry, R. A., & Kingsford, C. (2017). Salmon provides fast and bias-aware quantification of transcript expression. *Nature Methods*, *14*(4), 417–419. https://doi.org/10.1038/nmeth.4197

Pena-Blanco, A., & Garcia-Saez, A. J. (2018). Bax, Bak and beyond - mitochondrial performance in apoptosis. *The FEBS Journal*, *285*(3), 416–431. https://doi.org/10.1111/febs.14186

Peng, Y., Wang, L., Qing, Y., Li, C., Ren, T., Li, Q., ... Wang, D. (2015). Polymorphisms of BCL2 and BAX genes associate with outcomes in advanced non-small cell lung cancer patients treated with platinum-based chemotherapy. *Scientific Reports*, *5*, 17766. https://doi.org/10.1038/srep17766

Petrelli, B., Weinberg, J., & Hicks, G. G. (2018). Effects of prenatal alcohol exposure (PAE): Insights into FASD using mouse models of PAE. *Biochemistry and Cell Biology*, *96*(2), 131–147. https://doi.org/10.1139/bcb-2017-0280

Pham, C. T., MacIvor, D. M., Hug, B. A., Heusel, J. W., & Ley, T. J. (1996). Long-range disruption of gene expression by a selectable marker cassette. *Proceedings of the National Academy of Sciences of the United States of America*, *93*(23), 13090–13095. https://doi.org/10.1073/pnas.93.23.13090

Raudvere, U., Kolberg, L., Kuzmin, I., Arak, T., Adler, P., Peterson, H., & Vilo, J. (2019). G:Profiler: A web server for functional enrichment analysis and conversions of gene lists (2019 update). *Nucleic Acids Research*, *47*(W1), W191–W198. https://doi.org/10.1093/nar/gkz369

Robinson, A. M., Conley, D. B., & Kern, R. C. (2003). Olfactory neurons in bax knockout mice are protected from bulbectomy-induced apoptosis. *Neuroreport*, *14*(15), 1891–1894. https://doi.org/10.1097/00001756-200310270-00002

Sato, M., Suemori, H., Hata, N., Asagiri, M., Ogasawara, K., Nakao, K., ... Taniguchi, T. (2000). Distinct and essential roles of transcription factors IRF-3 and IRF-7 in response to viruses for IFN-alpha/beta gene induction. *Immunity*, *13*(4), 539–548. https://doi.org/10.1016/s1074-7613(00)00053-4

Saxena, A., Moshynska, O., Sankaran, K., Viswanathan, S., & Sheridan, D. P. (2002). Association of a novel single nucleotide polymorphism, G(−248)a, in the 5'-UTR of BAX gene in chronic lymphocytic leukemia with disease progression and treatment resistance. *Cancer Letters*, *187*(1–2), 199–205. https://doi.org/10.1016/s0304-3835(02)00378-6

Semaan, S. J., Li, Y., & Nickells, R. W. (2010). A single nucleotide polymorphism in the Bax gene promoter affects transcription and influences retinal ganglion cell death. *ASN Neuro*, *2*(2), e00032. https://doi.org/10.1042/AN20100003

Shannon, P., Markiel, A., Ozier, O., Baliga, N. S., Wang, J. T., Ramage, D., ... Ideker, T. (2003). Cytoscape: A software environment for integrated models of biomolecular interaction networks. *Genome Research*, *13*(11), 2498–2504. https://doi.org/10.1101/gr.1239303

Shi, J., Parada, L. F., & Kernie, S. G. (2005). Bax limits adult neural stem cell persistence through caspase and IP3 receptor activation. *Cell Death and Differentiation*, *12*(12), 1601–1612. https://doi.org/10.1038/sj.cdd.4401676

Streissguth, A. P., Aase, J. M., Clarren, S. K., Randels, S. P., LaDue, R. A., & Smith, D. F. (1991). Fetal alcohol syndrome in adolescents and adults. *JAMA*, *265*(15), 1961–1967.

Streissguth, A. P., & Dehaene, P. (1993). Fetal alcohol syndrome in twins of alcoholic mothers: Concordance of diagnosis and IQ. *American Journal of Medical Genetics*, *47*(6), 857–861. https://doi.org/10.1002/ajmg.1320470612

Subramanian, A., Tamayo, P., Mootha, V. K., Mukherjee, S., Ebert, B. L., Gillette, M. A., … Mesirov, J. P. (2005). Gene set enrichment analysis: A knowledge-based approach for interpreting genome-wide expression profiles. *Proceedings of the National Academy of Sciences of the United States of America*, *102*(43), 15545–15550. https://doi.org/10.1073/pnas.0506580102

Sulik, K. K. (1984). Critical periods for alcohol teratogenesis in mice, with special reference to the gastrulation stage of embryogenesis. *CIBA Foundation Symposium*, *105*, 124–141. https://doi.org/10.1002/9780470720868.ch8

Sulik, K. K., Cook, C. S., & Webster, W. S. (1988). Teratogens and craniofacial malformations: Relationships to cell death. *Development*, *103*(Suppl), 213–231.

Sulik, K. K., Johnston, M. C., & Webb, M. A. (1981). Fetal alcohol syndrome: Embryogenesis in a mouse model. *Science*, *214*(4523), 936–938.

Sun, L., Wei, L., Wei, L., & Li, D. (2018). Correlation between Bax gene polymorphisms and esophagus cancer. *Oncology Letters*, *16*(6), 7097–7101. https://doi.org/10.3892/ol.2018.9511

Sun, W., & Oppenheim, R. W. (2003). Response of motoneurons to neonatal sciatic nerve axotomy in Bax-knockout mice. *Molecular and Cellular Neurosciences*, *24*(4), 875–886. https://doi.org/10.1016/s1044-7431(03)00219-7

Voss, A. K., & Strasser, A. (2020). The essentials of developmental apoptosis. *F1000Research*, *9*. https://doi.org/10.12688/f1000research.21571.1

West, D. B., Engelhard, E. K., Adkisson, M., Nava, A. J., Kirov, J. V., Cipollone, A., … Lloyd, K. C. (2016). Transcriptome analysis of targeted mouse mutations reveals the topography of local changes in gene expression. *PLoS Genetics*, *12*(2), e1005691. https://doi.org/10.1371/journal.pgen.1005691

White, F. A., Keller-Peck, C. R., Knudson, C. M., Korsmeyer, S. J., & Snider, W. D. (1998). Widespread elimination of naturally occurring neuronal death in Bax-deficient mice. *The Journal of Neuroscience*, *18*(4), 1428–1439.

Wieczorek, L., Fish, E. W., O'Leary-Moore, S. K., Parnell, S. E., & Sulik, K. K. (2015). Hypothalamic-pituitary-adrenal axis and behavioral dysfunction following early binge-like prenatal alcohol exposure in mice. *Alcohol*, *49*(3), 207–217. https://doi.org/10.1016/j.alcohol.2015.01.005

Young, C., Klocke, B. J., Tenkova, T., Choi, J., Labruyere, J., Qin, Y. Q., … Olney, J. W. (2003). Ethanol-induced neuronal apoptosis in vivo requires BAX in the developing mouse brain. *Cell Death and Differentiation*, *10*(10), 1148–1155. https://doi.org/10.1038/sj.cdd.4401277

Zhang, C., Ojiaku, P., & Cole, G. J. (2013). Forebrain and hindbrain development in zebrafish is sensitive to ethanol exposure involving agrin, Fgf, and sonic hedgehog function. *Birth Defects Research. Part A, Clinical and Molecular Teratology*, *97*(1), 8–27. https://doi.org/10.1002/bdra.23099

SUPPORTING INFORMATION

Additional supporting information may be found in the online version of the article at the publisher's website.

How to cite this article: Fish, E. W., Mendoza-Romero, H. N., Love, C. A., Dragicevich, C. J., Cannizzo, M. D., Boschen, K. E., Hepperla, A., Simon, J. M., & Parnell, S. E. (2022). The pro-apoptotic *Bax* gene modifies susceptibility to craniofacial dysmorphology following gastrulation-stage alcohol exposure. *Birth Defects Research*, 1–15. https://doi.org/10.1002/bdr2.2009